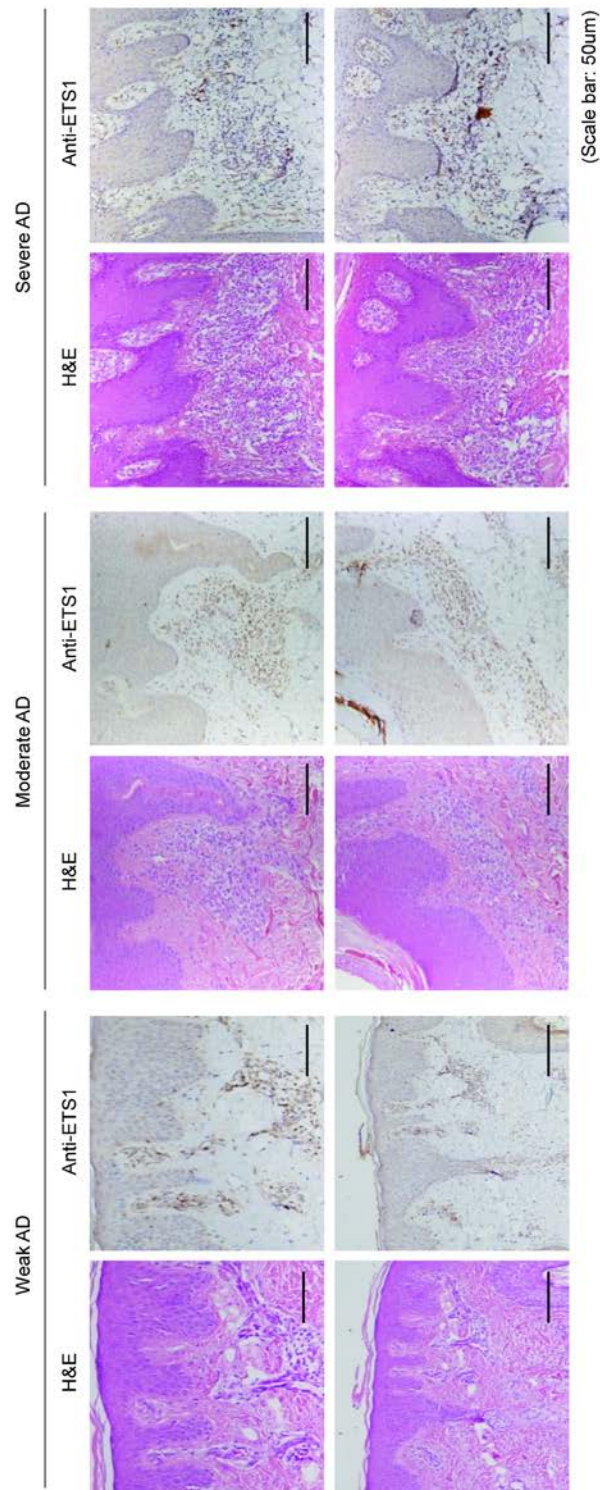
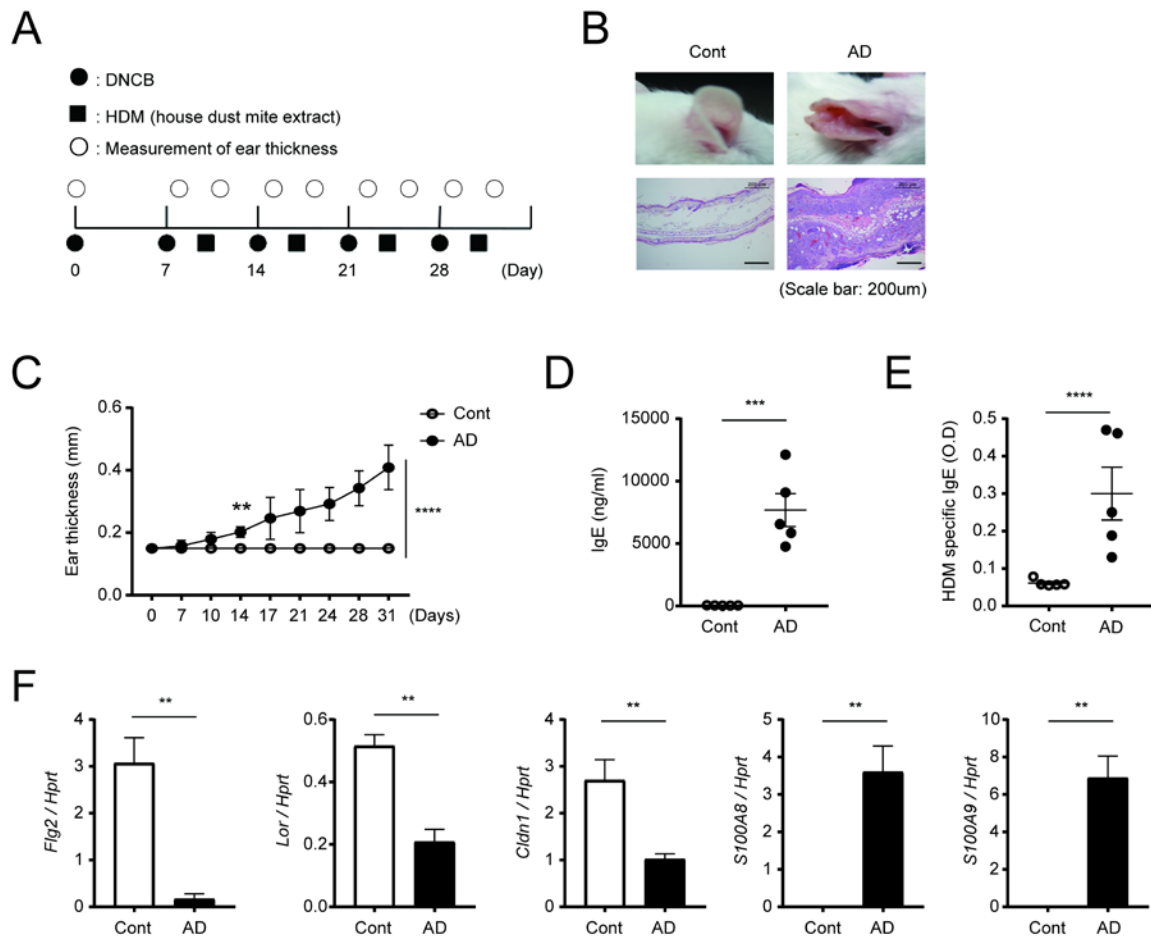


Supplemental Figure 1



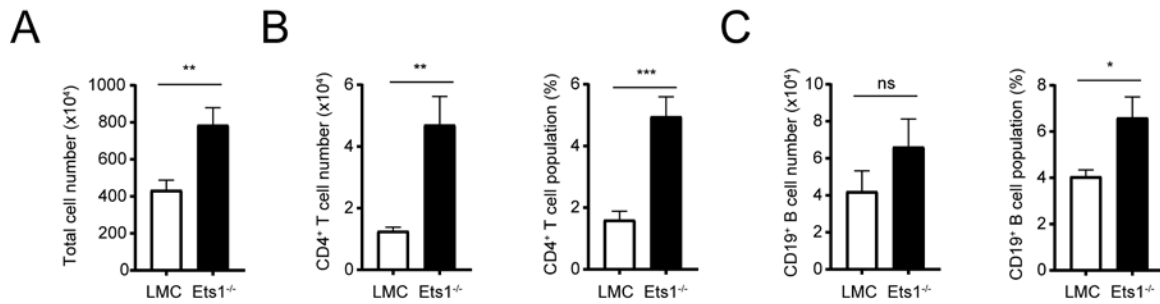
Supplemental Figure 1. Hematoxylin and eosin (H&E) staining of the human skin biopsies. These are larger representative images of Figure 1A. Hematoxylin and eosin (H&E) staining of the human skin biopsies confirmed the clinical diagnoses of weak, moderate, and severe atopic dermatitis (AD), respectively. Ets1+ lymphocytes were analyzed by immunohistochemistry (IHC) using anti-Ets1 with the same specimen from H&E.

Supplemental Figure 2



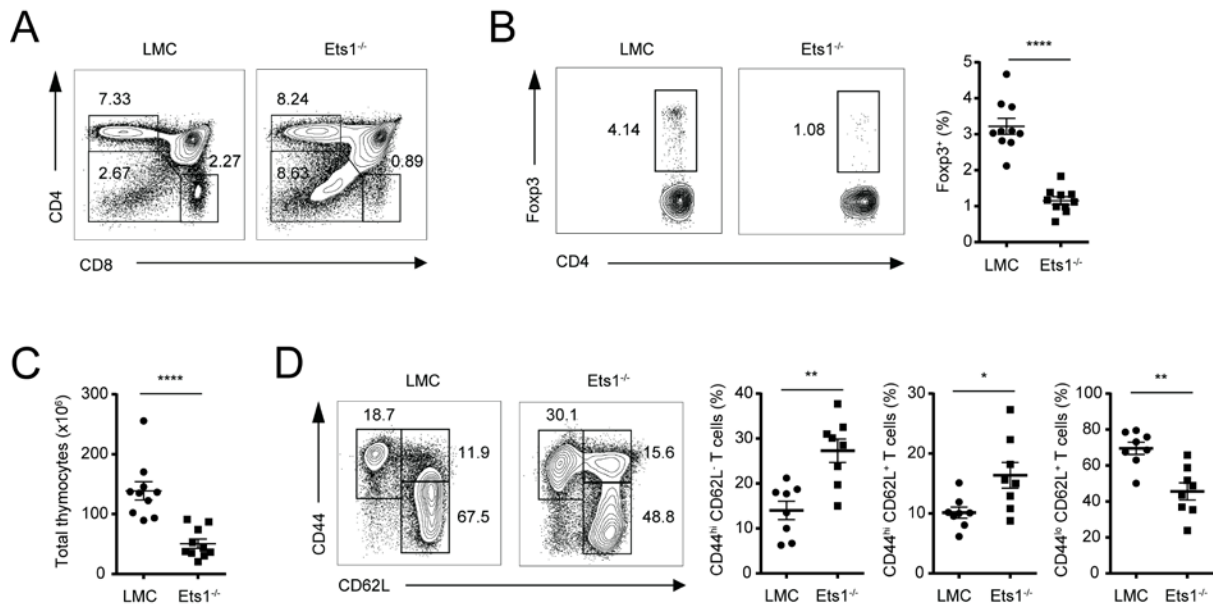
Supplemental Figure 2. Induction of experimental AD in BALB/c mice. (A) Schematic diagram of the experimental AD induction by hapten (DNCB) and house dust mite extract (HDM). (B) Representative photographs of mouse ears from each group (upper) and H&E staining of the ear biopsies (lower) confirmed the clinical symptoms of AD. (C) Ear thickness during the course of AD was measured 24hr after DNCB or HDM extract application by using a dial thickness gauge. The data are expressed as mean \pm SD. **, $p \leq 0.005$; ****, $p \leq 0.0001$ (from day 17 to 31); two-way ANOVA. (D) The total IgE and (E) HDM allergen-specific IgE levels in serum from the mouse groups were measured by ELISA. (F) RNA was collected from the cells of ear tissues and the relative levels of *filaggrin*, *loricrin*, *claudin*, *S100A8* and *S100A9* were evaluated by qRT-PCR. Data represent results from three independent experiments. Error bars represent the mean \pm SEM. **, $p \leq 0.005$; ***, $p \leq 0.0005$; ****, $p \leq 0.0001$; Student's t test.

Supplemental Figure 3



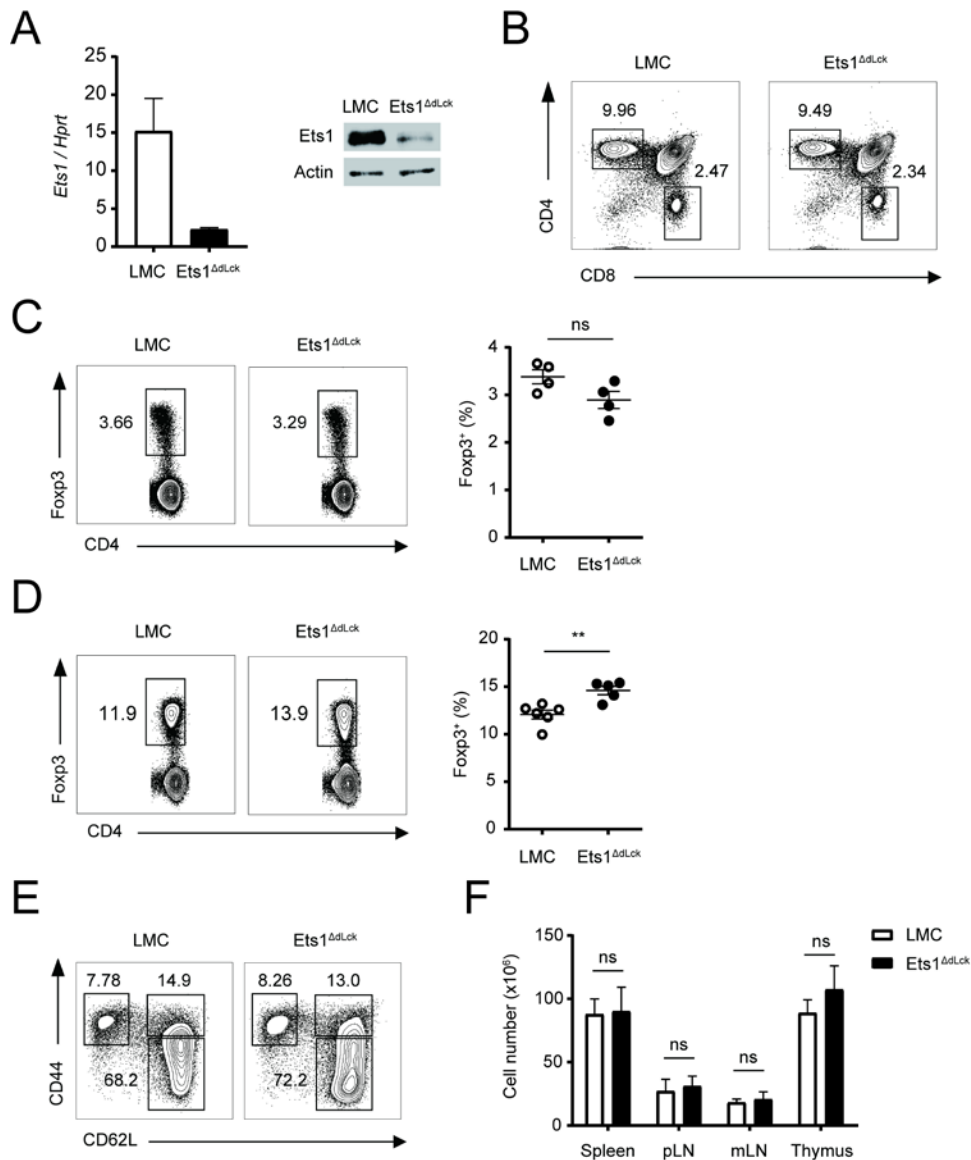
Supplemental Figure 3. Analysis of infiltrated immune cells at the inflamed ear tissues. (A) Cells from the ear tissues were collected from LMC and Ets1^{-/-} mice under AD, and absolute number and frequency of (B) CD4⁺ T cells and (C) CD19⁺ B cells from the ear tissues were calculated. Data represent results from three independent experiments. Error bars represent the mean ± SEM. ns, not significant; **, $p \leq 0.005$; ***, $p \leq 0.0005$; Student's t test.

Supplemental Figure 4



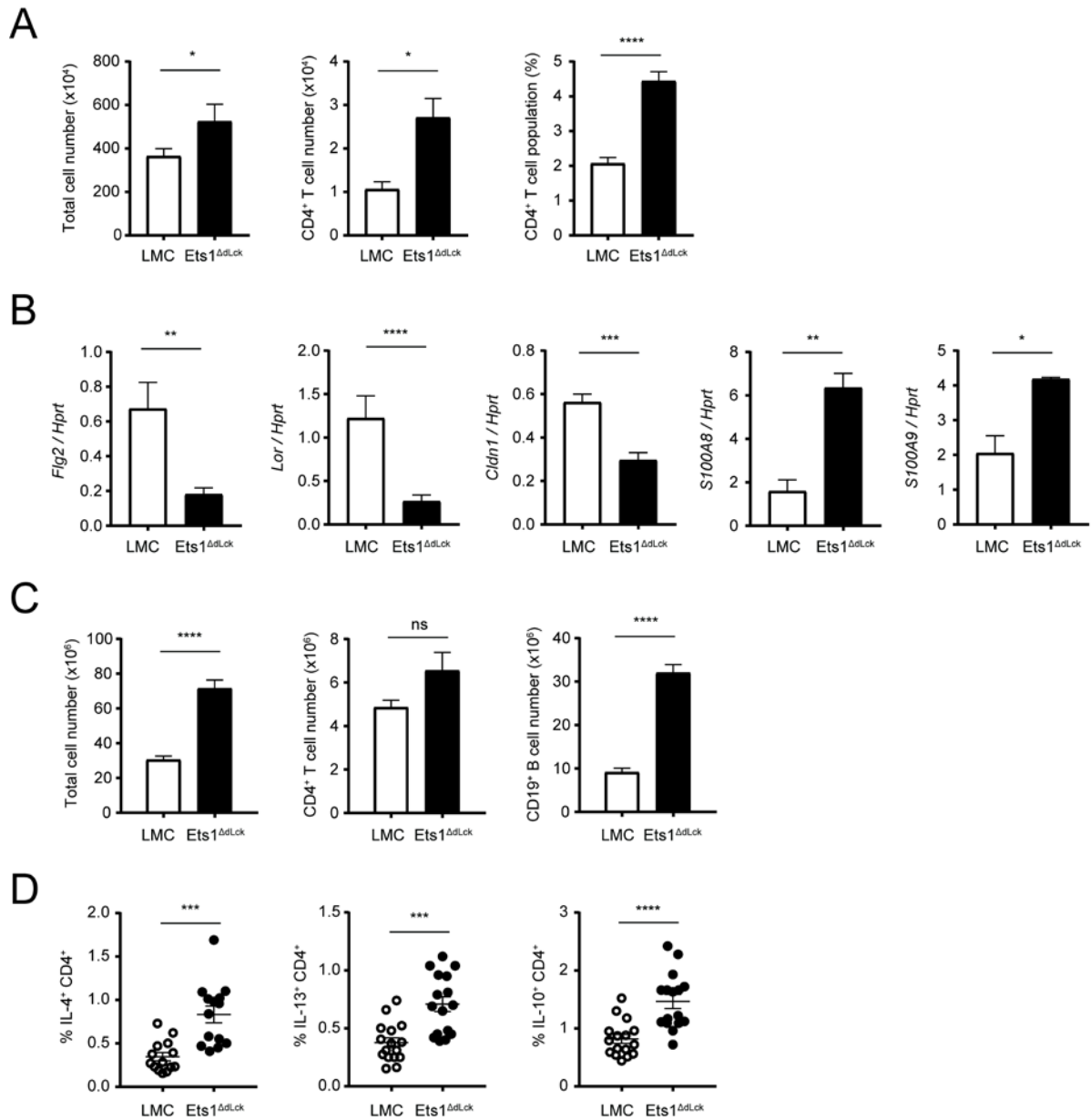
Supplemental Figure 4. Analysis of *Ets1* germline knockout (*Ets1*^{-/-}) mice under homeostatic conditions. (A) Thymic profile of single positive CD4⁺ and CD8⁺ T cells from the LMC and *Ets1*^{-/-} mice were analyzed by flow cytometry. (B) Foxp3⁺ regulatory T (Treg) cells from CD4SP in the thymus were analyzed. (C) Cells from the thymus were calculated and compared. (D) Activated/memory and naïve frequency of CD4⁺ T cells from the LNs were analyzed by CD62L and CD44 expression. Error bars represent the mean ± SEM. ns, not significant; *, $p \leq 0.05$; **, $p \leq 0.005$; ***, $p \leq 0.0005$; ****, $p \leq 0.0001$; Student's t test. Representative plot comes from the analysis of four to six individual mice.

Supplemental Figure 5



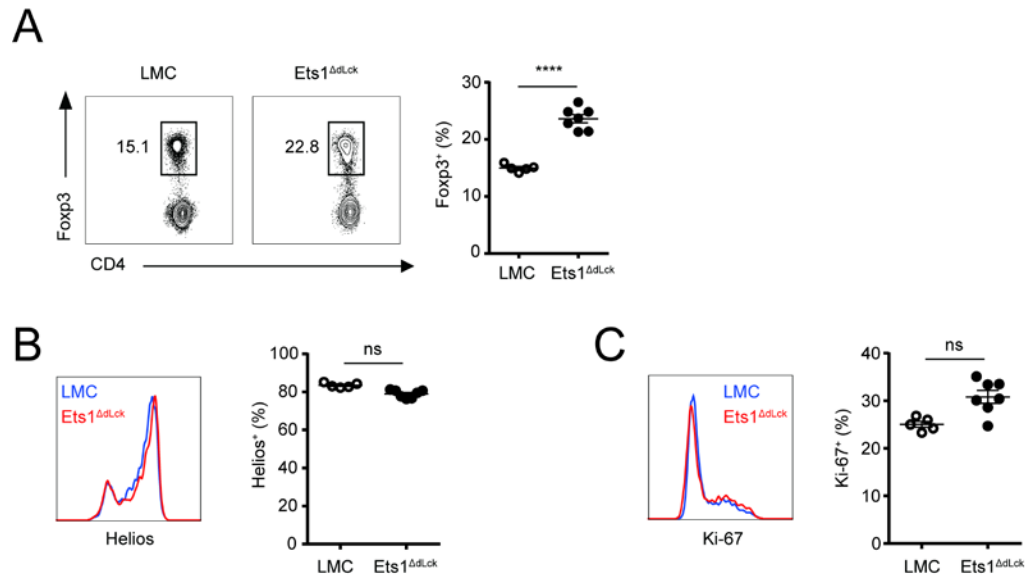
Supplemental Figure 5. Analysis of distal-*Lck-cre* (*Ets1*^{ΔdLck}) mice under homeostatic conditions. (A) *Ex vivo* isolated CD4⁺ T cells from the skin-draining LNs in the periphery were isolated using a CD4⁺ negative selection method. RNA was collected from the cells and the relative level of *Ets1* was evaluated by qRT-PCR. Protein levels of *Ets1* and Actin expression were examined by immunoblotting. (B) Thymic profile of single positive CD4⁺ and CD8⁺ T cells from the LMC and *Ets1*^{ΔdLck} mice were analyzed by flow cytometry. Fcγp3⁺ regulatory T (Treg) cells in the thymus (C) and peripheral LNs (D) were analyzed by flow cytometry. (E) Activated/memory and naïve frequency of CD4⁺ T cells from the LNs were analyzed by CD62L and CD44 expression. (F) Cells from the different lymphoid tissues were calculated and compared. Error bars represent the mean ± SEM. ns, not significant; **, $p \leq 0.005$; Student's t test. Representative plot comes from the analysis of four to six individual mice.

Supplemental Figure 6



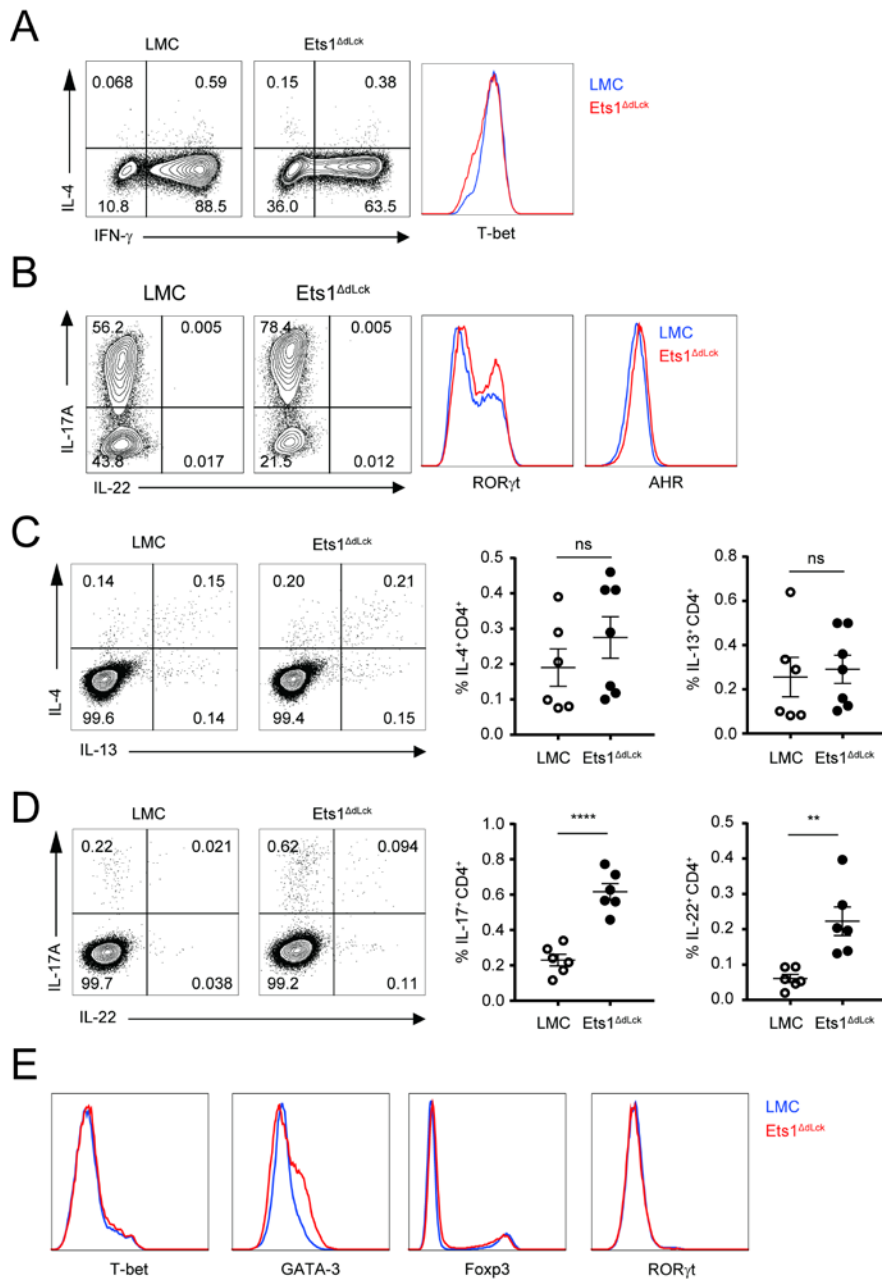
Supplemental Figure 6. Analysis of LMC and Ets1^{ΔdLck} mice under AD condition. (A) Cells from the ear tissues were collected from LMC and Ets1^{ΔdLck} mice under AD, and absolute number and frequency of CD4⁺ T cells were calculated. (B) RNAs were collected from the cells of ear tissues and the relative levels of *filaggrin*, *loricrin*, *claudin*, *S100A8* and *S100A9* were evaluated by qRT-PCR. (C) Cells from the skin-draining LNs were collected and absolute number of total, CD4⁺ T and CD19⁺ B cells was calculated. (D) Intracellular staining of IL-4, IL-13 and IL-10 by CD4-gated T cells were analyzed. Data represent results from three independent experiments. Error bars represent the mean ± SEM. ns, not significant; *, $p \leq 0.05$; **, $p \leq 0.005$; ***, $p \leq 0.0005$; ****, $p \leq 0.0001$; Student's t test.

Supplemental Figure 7



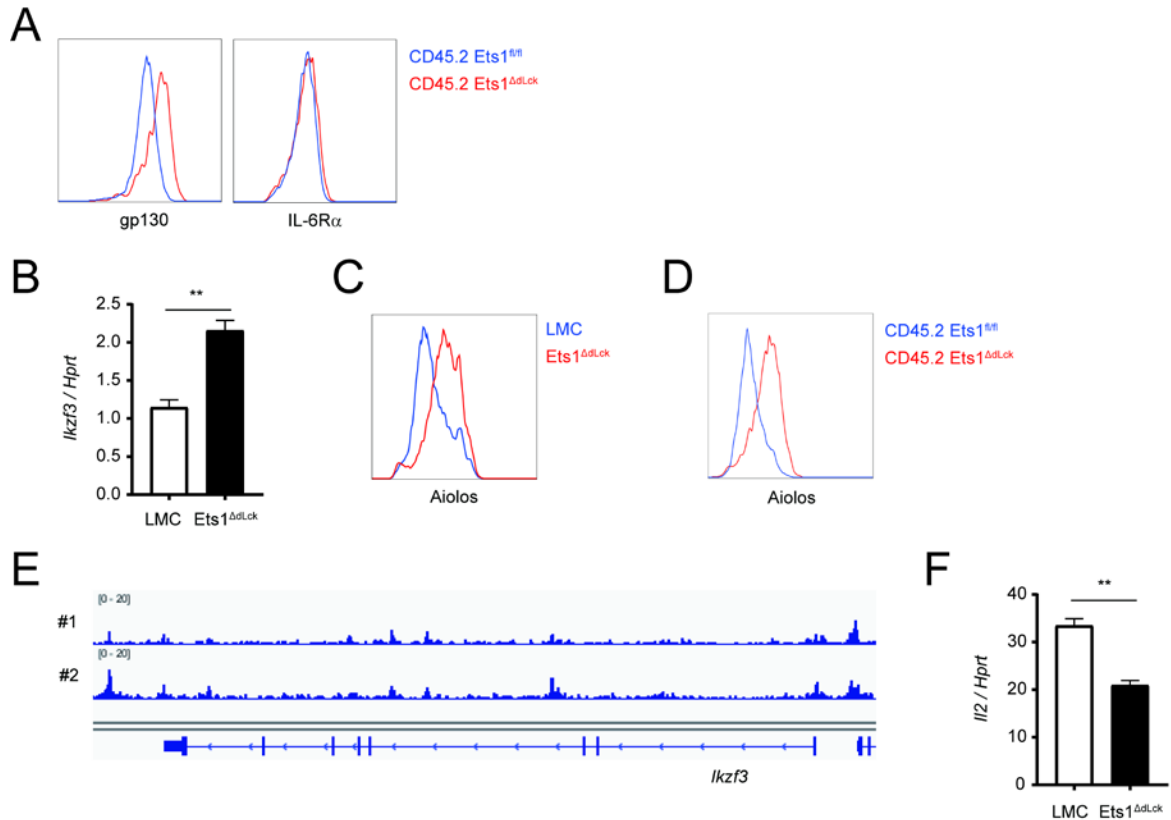
Supplemental Figure 7. Analysis of Treg cells from distal-*Lck*-cre (*Ets1*^{ΔdLck}) mice under AD-like skin inflammation. (A) Fcγp3⁺ regulatory T (Treg) cells in the skin-draining LNs were analyzed by flow cytometry. Protein levels of Helios (B) and Ki-67 (C) in CD4⁺Fcγp3⁺ Treg cells under the diseased condition were examined. Error bars represent the mean \pm SEM. ns, not significant; ****, $p \leq 0.0001$; Student's t test. Representative plot comes from the analysis of five to seven individual mice.

Supplemental Figure 8



Supplemental Figure 8. Analysis of *in vitro* Th cell differentiation and *ex vivo* CD4⁺ T cells from LMC and Ets1^{ΔdLck} mice. (A and B) Naïve CD4⁺ T cells from LMC and Ets1^{ΔdLck} mice were cultured 3-4 days with plate-bound anti-CD3 and anti-CD28 in the presence of skewing cytokines IL-12 and anti-IL-4 for Th1 (A) and IL-6, TGF- β 1, anti-IL-4 and anti-IL-12 for conventional Th17 differentiation. Expression of the indicated cytokines and transcription factors were analyzed by flow cytometry. (C and D) *Ex vivo* isolated total lymphocytes from skin-draining LNs were given PMA and ionomycin stimulation with GolgiStop or GolgiPlug for 4hr. Intracellular staining of IL-4, IL-13, IL-17A and IL-22 by CD4-gated T cells were analyzed. (E) Expression of the indicated transcription factors were analyzed using *ex vivo* CD4⁺ T cells from LMC and Ets1^{ΔdLck} mice. Error bars represent the mean \pm SEM. ns, not significant; **, $p \leq 0.005$; ****, $p \leq 0.0001$; Student's t test. Representative plot comes from the analysis of six individual mice.

Supplemental Figure 9



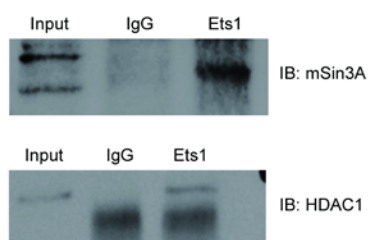
Supplemental Figure 9. Analysis of gp130 and *Ikzf3* (Aiolos) expression in mixed BM chimeras and *Ets1* ^{Δ dLck} mice. (A) Bone marrow cells from LMC or *Ets1* ^{Δ dLck} mice were mixed with BM cells from congenic CD45.1 wild-type (WT) mice at the 1:1 ratio. At 6 to 8 weeks after BM cell transfer, cells from LNs were analyzed by flow cytometry. Protein level of *Il6st* (gp130) and *Il6ra* (IL-6R α) was examined by surface staining. (B) *Ikzf3* mRNA and (C) intracellular Aiolos expression were analyzed in the naïve CD4⁺ T cells from LMC and *Ets1* ^{Δ dLck} mice. (D) Intracellular Aiolos expression from mixed BM chimera was analyzed in the CD4⁺ T cells from CD45.2 LMC and CD45.2 *Ets1* ^{Δ dLck} mice. (E) Ets1 ChIP-seq confirmed binding of Ets1 in regulatory elements of *Ikzf3* locus. Numbers represent two different sets of data. (F) Naïve CD4⁺ T cells from LMC and *Ets1* ^{Δ dLck} mice were stimulated with PMA and ionomycin for 4 hours, then *Il2* mRNA level normalized with *Hprt* was evaluated by qRT-PCR. Representative plot comes from the analysis of four to six individual mice. Error bars represent the mean \pm SEM. **, $p \leq 0.005$; Student's t test. Representative plot comes from the analysis of four to six individual mice.

Supplemental Figure 10

A

Accession-ID	Protein Name	Official full name
IPI00408803	Suds3	SDS3 homolog, SIN3A corepressor complex component
IPI00117932	Sin3a	SIN3 transcription regulator family member A
IPI00776411	Hcfc1	host cell factor C1
IPI00114232	Hdac1	histone deacetylase 1

B



Supplemental Figure 10. Ets1 suppresses its target genes by interacting with transcriptional repressors. Immunoprecipitation with anti-Ets1 was performed with *ex vivo* CD4⁺ T cells and LC-MS/MS analysis was performed. (A) Indicated proteins were selected based on the detected peptide numbers in three independent experiments. (B) After co-immunoprecipitation of Ets1, direct interaction of Ets1 with transcriptional repressor complex (HDAC1 and mSin3A) was confirmed by immunoblotting.